

LA-UR-

*Approved for public release;
distribution is unlimited.*

Title:

Author(s):

Intended for:



Los Alamos National Laboratory, an affirmative action/equal opportunity employer, is operated by the Los Alamos National Security, LLC for the National Nuclear Security Administration of the U.S. Department of Energy under contract DE-AC52-06NA25396. By acceptance of this article, the publisher recognizes that the U.S. Government retains a nonexclusive, royalty-free license to publish or reproduce the published form of this contribution, or to allow others to do so, for U.S. Government purposes. Los Alamos National Laboratory requests that the publisher identify this article as work performed under the auspices of the U.S. Department of Energy. Los Alamos National Laboratory strongly supports academic freedom and a researcher's right to publish; as an institution, however, the Laboratory does not endorse the viewpoint of a publication or guarantee its technical correctness.

Adaptation of the Multistage Preequilibrium Model for the Monte Carlo Method (I)

R. E. Prael (X-6) and Michael Bozoian (T-2)
Los Alamos National Laboratory
Los Alamos, NM 87545

September 30, 1988

Abstract

A Monte Carlo formulation of the multistage preequilibrium model (MPM) for particle emission from a compound nucleus is described. Although the long-term goal of the effort is to provide an additional physics model for the Monte Carlo code HETC, connecting the intranuclear cascade model and the evaporation model, the present work is implemented as a stand-alone Monte Carlo code, PREEQ1, which illustrates the method and tests the algorithms.

Introduction

The Monte Carlo transport code HETC [1], widely used for computations in medium energy particle physics, employs an intranuclear cascade model to describe the reaction process. The cascade model, which treats the reaction as a series of multiple quasi-free scattering events from two-body interactions, is largely effective above 100 MeV. At lower incident particle energies, the purely two-body picture shows considerable limitation.

The long-term objective of this work is to adapt the exciton preequilibrium model [2],[3] to a Monte Carlo format which may be used in HETC to replace the intranuclear cascade at low energies and, at higher energies, to supplement the intranuclear cascade as a subsequent preequilibrium emission model before application of the evaporation model. In the present paper, we outline the development of such a Monte Carlo model and describe its implementation in a stand-alone testing code, PREEQ1. Two issues in particular are *not* addressed in this paper: the final choice of a model for calculating inverse reaction cross sections and the method for interfacing the model with the existing intranuclear cascade model.

The form of the exciton model which we consider is frequently termed “the multistage preequilibrium model” (MPM) in that it may predict the emission of one or more particles before assuming that the nuclear system has approached equilibrium and thus is better described by a statistical model (the evaporation model in HETC). In our development, we have obtained guidance from three code implementations of the MPM: GNASH [4], PRECO [5], and GRYPHON [6]. Models and methods used in these “analytical” codes have been supplemented by techniques peculiar to the Monte Carlo method or dictated by considerations of computing efficiency when using the Monte Carlo method.

Notation

The appropriate variables for characterizing a nuclear state in the multistage preequilibrium model (MPM) are the mass and charge numbers A and Z , the particle and hole numbers P and H , and excitation energy E . The exciton number N is given by $N = P + H$. It is then convenient to define a exciton state variable C by

$$C \equiv (A, Z, P, H)$$

so that we can define our nuclear state by the pair (C, E) .

Within the MPM, we have two classes of possible transitions. The first involves the emission of a particle of type b from the state (C, E) :

$$(C, E) \xrightarrow{b} (C - b, E - S_b - \epsilon_b) = (C', E')$$

where S_b is the separation energy for particle b , ϵ_b is the kinetic energy emitted in the center of mass for the transition, and

$$C - b \equiv (A - a_b, Z - z_b, P - a_b, H)$$

where a_b and z_b are the mass and charge numbers of particle b . It is also convenient to define $C + b \equiv (A + a_b, Z + z_b, P + a_b, H)$ to label a possible precursor of C .

The second type of transition allowed corresponds to $\Delta N = +2$ without a change in any other state variable. It is convenient to use the following notation for such cases:

$$(C, E) \xrightarrow{\Delta N=2} (C + 2, E)$$

$$(C - 2, E) \xrightarrow{\Delta N=2} (C, E)$$

where

$$C \pm 2j \equiv (A, Z, P \pm j, H \pm j) .$$

A further notational simplification will be used with respect to energy integrals. Let $f(\epsilon_b)$ be an arbitrary function of the emission energy ϵ_b . Then we define

$$\int f(\epsilon_b)d\epsilon_b \equiv \int_{\epsilon_{cb}}^{E-S_b} f(\epsilon_b)d\epsilon_b$$

to be the integral over the entire range $\epsilon_{cb} \leq \epsilon_b \leq E - S_b$ allowed by conservation of energy for excitation E and constrained by a possible Coulomb barrier ϵ_{cb} . Similarly, an integral over excitation energy without specified limits of integration is assumed to be an integral over all excitations energies where the integrand satisfies all such appropriate constraints.

The Master Equation

Let us make the following definitions:

- $q_\nu(C, E, t)$ is the *population density per unit excitation energy* of state C at excitation energy E at time t in the ν stage of the multistage process, given that the nuclear system begins at $t = 0$ in stage $\nu = 1$ with state C_0 and excitation E_0 ;
- $\lambda^+(C, E)$ and $\lambda^-(C, E)$ are the *internal transition rates* for $\Delta N = +2$ and $\Delta N = -2$ transitions respectively;
- $W(C, E)$ is the *total emission rate* of all outgoing particles at all energies (leading to the population of stage $\nu + 1$);
- $\mathcal{S}_\nu(C, E, t)$ is the rate that the state (C, E) is being populated per unit excitation energy by transitions from the $\nu - 1$ stage.

Then the time dependent master equation for the ν stage may be written as

$$\begin{aligned} dq_\nu(C, E, t)/dt = & \lambda^+(C - 2, E)q_\nu(C - 2, E, t) + \lambda^-(C + 2, E)q_\nu(C + 2, E, t) \\ & - [\lambda^+(C, E) + \lambda^-(C, E) + W(C, E)]q_\nu(C, E, t) + \mathcal{S}_\nu(C, E, t) \quad . \end{aligned} \quad (1)$$

The initial condition may then be defined by

$$q_\nu(C, E, t = 0) = \delta_{\nu,1}\delta_{C,C_0}\delta(E - E_0) \quad . \quad (2)$$

Let us make the further definitions:

- since we are considering a *pure preequilibrium model*, we consider the probability of $\Delta N = -2$ transitions to be negligible, and so $\lambda^-(C, E) \approx 0$ and will be ignored (see discussion below);

- $w_b(\epsilon, C, E)$ is the *emission rate spectrum* for the emission of particles of type b with emission energy ϵ from the state (C, E) and vanishing outside of the interval $\epsilon_{cb} \leq \epsilon \leq E - S_b$;
- $W_b(C, E) = \int w_b(\epsilon, C, E)d\epsilon$ is the *emission rate* for particles of type b ;
- $W(C, E) = \sum_b W_b(C, E)$ is the *total emission rate* over all outgoing particles and energies;
- $\tau(C, E) = [\lambda^+(C, E) + \lambda^-(C, E) + W(C, E)]^{-1} \approx [\lambda^+(C, E) + W(C, E)]^{-1}$ is the *transition time* for state (C, E) .

The source term into the state (C, E) in stage ν is then

$$\begin{aligned} S_\nu(C, E, t) &= \sum_b \int w_b(\epsilon, C + b, E + S_b + \epsilon) q_{\nu-1}(C + b, E + S_b + \epsilon, t) d\epsilon \\ &= \sum_b \int w_b(E' - S_b - E, C + b, E') q_{\nu-1}(C + b, E', t) dE' \end{aligned}$$

With the above definitions, we may may write equation 1 as

$$\begin{aligned} dq_\nu(C, E, t)/dt &= -q_\nu(C, E, t)/\tau(C, E) + \lambda^+(C - 2, E)q_\nu(C - 2, E, t) \\ &+ \sum_b \int w_b(E' - S_b - E, C + b, E') q_{\nu-1}(C + b, E', t) dE' \end{aligned} \quad (3)$$

The solution of (3) as a function of time is a sum of decaying exponentials. We can therefore define the time-independent function $Q_\nu(C, E)$ by the relation

$$\tau(C, E)Q_\nu(C, E) = \int_0^\infty q_\nu(C, E, t) dt \quad .$$

Furthermore,

$$\int_0^\infty \frac{dq_\nu(C, E, t)}{dt} dt = -q_\nu(C, E, t=0) = -\delta_{\nu,1} \delta_{C,C_0} \delta(E - E_0)$$

using equation 2. We may then integrate (3) over time to obtain the following set of three equations. First we have an initial condition

$$Q_1(C_0, E) = \delta(E - E_0) \quad (4)$$

where we have used the condition $q_1(C_0 - 2, E, t) \equiv 0$. Next we have the first stage ($\nu = 1$) equation for $C \neq C_0$:

$$Q_1(C, E) = \lambda^+(C - 2, E)\tau(C - 2, E)Q_1(C - 2, E) \quad . \quad (5)$$

Finally, for the subsequent stages ($\nu > 1$),

$$Q_\nu(C, E) = \lambda^+(C - 2, E)\tau(C - 2, E)Q_\nu(C - 2, E) + \sum_b \int w_b(E' - S_b - E, C + b, E')\tau(C + b, E')Q_{\nu-1}(C + b, E')dE' \quad (6)$$

where the source term includes contributions from all the populated states of the $\nu - 1$ stage which may reach the state (C, E) by the emission of some particle b . By inspection of equations 4, 5, and 6, we may interpret the function $Q_\nu(C, E)$ as follows:

- $Q_\nu(C, E)$ is the total population per unit excitation energy which has entered the state C in the ν stage from any source.

The form of the source term in (6) also indicates how the differential cross section for the emission of particle type b is to be determined from $Q_\nu(C, E)$:

$$\frac{d\sigma_b}{d\epsilon} = \sigma_R \sum_\nu \sum_C \int w_b(\epsilon, C, E)\tau(C, E)Q_\nu(C, E)dE \quad (7)$$

which includes the contributions from all stages (which we choose to consider) and all states (C, E) which become populated in each stage. The problem of obtaining the particle emission spectrum is thus reduced to obtaining a numerical solution for the function $Q_\nu(C, E)$ from the recursion relations of equations 4, 5, and 6. The process will be terminated after some state C_{max} is reached within each stage and will be terminated after some ν_{max} stages; all further emission is assumed to be obtainable from a statistical model for nuclear deexcitation.

The Monte Carlo Algorithm

It is apparent that equations 4, 5, and 6 can be interpreted as defining a random walk problem whereby we define the system to be in the initial state (C_0, E_0) and allow the state to evolve with the appropriate probabilities. Two possibilities suggest themselves as providing the initial condition:

- a projectile type, projectile energy, target nucleus, and assumed reaction cross section σ_R are defined and the initial condition is taken to be the $(P = 2, H = 1)$ in the compound nucleus so defined (the lowest order emitting state);
- the initial condition is defined from the residual nuclear state obtained from a single execution of a Monte Carlo intranuclear cascade calculation.

It is the latter case which we will employ by including a MPM calculation in HETC.

Since we are now treating the evolution of the nuclear system in a probabilistic manner, we redefine some of the quantities above in terms of discrete probabilities and probability densities:

- $P^+(C, E) = \lambda^+(C, E)\tau(C, E)$ is the probability of a $\Delta N = +2$ transition $(C, E) \longrightarrow (C + 2, E)$;
- $P_b(C, E) = W_b(C, E)\tau(C, E)$ is the probability of emitting a particle b from state (C, E) at any emission energy;
- $p_b(\epsilon, C, E) = w_b(\epsilon, C, E)/W_b(C, E)$ is the probability density function for the emission energy ϵ , *given* that b is emitted from (C, E) .

The analog random walk algorithm then takes the following form.

1. The initial condition of the system ($C = C_0, E = E_0$) is defined, as is the transformation from the center of mass (COM) system back to the laboratory system; the system is defined as being in stage $\nu = 1$.
2. A test is made to see if the system has already emitted from the maximum allowed stage or has evolved beyond the maximum exciton number allowed in the present stage; if so, the computation has concluded.
3. The transition probabilities P_b and $P^+ = 1 - \sum_b P_b$ are calculated; if the state reached is particle-stable, the computation has concluded.
4. A uniform random sampling is made to choose the transition type.
5. If the nonemitting $\Delta N = +2$ transition is selected, the state of the system is redefined by $C \longrightarrow C' = C + 2$ with E unchanged; the calculation returns to step 2 above.
6. If emission of particle b is selected, the emission energy ϵ is obtained by sampling from the probability density function $p_b(\epsilon, C, E)$.
7. The emission energy ϵ is partitioned between the emitted particle and the recoiling nucleus, and the emission angle in the COM is randomly selected from an isotropic distribution or from the parameterization of Kalbach described below.
8. The kinematic variables of the emitted particle are computed in the laboratory frame and so recorded; the kinematic variables of the recoiling nucleus are recalculated and a new COM-to-lab transformation determined.

9. The state of the nuclear system is redefined by $(C, E) \longrightarrow (C', E') = (C - b, E - S_b - \epsilon)$; the calculation returns to step 2 above.

At the conclusion of the process, the final nuclear state (A, Z, E) , together with the kinematic parameters for nuclear recoil, is recorded as an initial condition for a subsequent statistical deexcitation calculation such as the evaporation model employed in HETC.

The Particle Emission Rate

We take the emission rate spectrum for the emission of particle b from (C, E) to be [6]

$$w_b(\epsilon, C, E) = \frac{(2s_b + 1)}{\pi^2 \hbar^3} \mu_b \epsilon \sigma_b(\epsilon) \frac{\omega(C - b, E')}{\omega(C, E)} Q_b \quad . \quad (8)$$

In equation 8,

- s_b and μ_b are the intrinsic spin and reduced mass of the ejectile;
- σ_b is the inverse reaction cross section;
- ϵ is the channel energy in the decay channel;
- $E' = E - S_b - \epsilon$ is the excitation energy of the residual nucleus;
- $\omega(C, E)$ is the level density of the emitting nucleus;
- $\omega(C - b, E')$ is the level density of the residual nucleus.

Q_b is a factor which reflects the correlation of the emission process with the incident projectile and the effect of proton-neutron distinguishability [3].

For the inverse cross section $\sigma_b(\epsilon)$, we tentatively employ the geometric cross section of reference [5] with a Coulomb barrier penetration factor $T_b(\epsilon)$:

$$\sigma_b(\epsilon) = \pi(\mathcal{R}A_r^{1/3} + R_b + \chi(\epsilon))^2 T_b(\epsilon) \quad (9)$$

where

- A_r is the mass number of the potential residual nucleus;
- $\mathcal{R} = 1.23$ fm;
- $R_b = 0$ for $b = n, p$;
- $R_b = 0.8$ fm for $b = d, t, \tau$;

- $R_b = 1.2$ fm for $b = \alpha$;
- $\chi(\epsilon)$ is the (nonrelativistic) reduced channel wavelength;
- $T_n(\epsilon) = 1$ for neutrons.

The Coulomb barrier penetration factor is given by

$$T_b(\epsilon) = (1 - k_b V_b / \epsilon) \quad (10)$$

with the Coulomb energy V_b given by

$$V_b = \frac{z_b(Z - z_b)e^2}{\mathcal{R}_c A_r^{1/3} + R_b} \quad \text{for } \mathcal{R}_c = 1.70 \text{ fm.}$$

The factors $k_b < 1$ reflect barrier penetration and are obtained from a parameterization of the s-wave Coulomb barrier transmission factor at the condition $\epsilon = V_b$.

When equation 10 is used, we obtain a cutoff energy for the charged particle integrations given by $\epsilon_{cb} = k_b V_b$. Let us define for charged particles

$$\begin{aligned} \beta_b &= -\epsilon_{cb} \\ \tilde{\sigma}_b &= \pi(\mathcal{R}A_r^{1/3} + R_b + \chi(\epsilon)_{cb})^2 \\ \Phi_b(\epsilon) &= \left[\frac{\mathcal{R}A_r^{1/3} + R_b + \chi(\epsilon)}{\mathcal{R}A_r^{1/3} + R_b + \chi(\epsilon_{cb})} \right]^2. \end{aligned}$$

For purposes of computation, we approximate

$$\sigma_b(\epsilon)T_b(\epsilon) \approx \tilde{\sigma}_b(1 + \beta_b/\epsilon) \quad (11)$$

to perform the computation of the emission probability, and then apply Φ_b as a Monte Carlo rejection factor to correct for our approximation. For the neutron channel, we may also apply the approximation (11); however, for neutrons, we define

$$\begin{aligned} \epsilon_{cn} &= 0 \\ r_0 &= \mathcal{R}A_r^{1/3} \\ \beta_n &= \frac{\hbar^2 c^2}{2\mu_n r_0^2} \\ \tilde{\sigma}_n &= 2\pi r_0^2 \\ \Phi_n(\epsilon) &= \frac{1}{2} \frac{(r_0 + \chi(\epsilon))^2}{r_0^2(1 + \beta_n/\epsilon)} \end{aligned}$$

where $r_0^2 \beta_n / \epsilon = \chi^2(\epsilon)$.

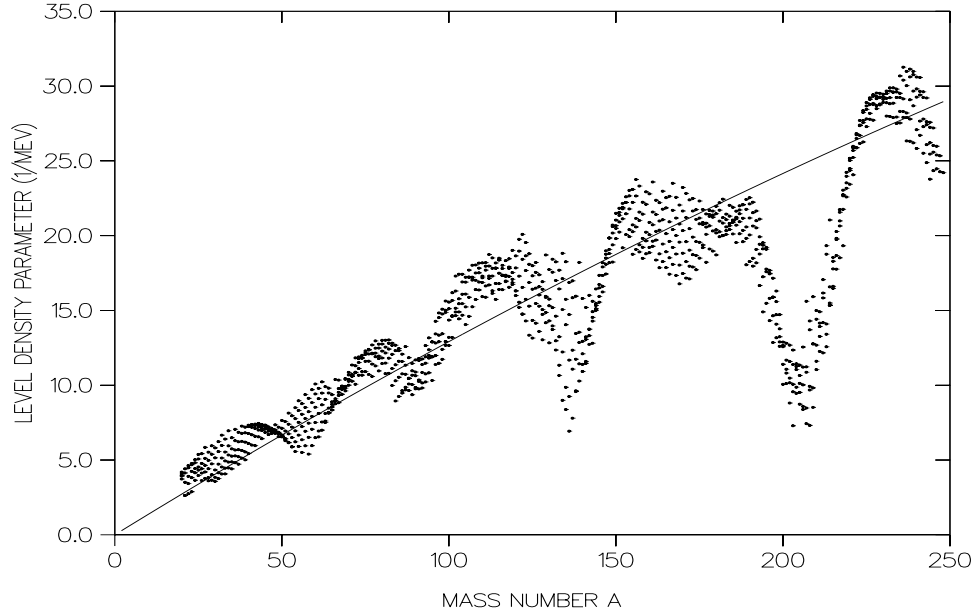


Figure 1: Level density parameter model. Solid line – high excitation limit, points – low excitation limit for nuclei near the line of stability.

The level density formulation employed is that of Williams [7]:

$$\omega(C, E) = \frac{g^N [E - A(P, H)]^{N-1}}{P!H!(N-1)!} \quad (12)$$

where g is the single-particle level density parameter, related to the parameter a of the Fermi gas level density $\omega_{FG} \propto \exp(2\sqrt{aU})$ by $a = \pi^2 g/6$. To obtain g , we use the energy dependent formulation of Ignatyuk [8] as implemented in GNASH [4], with the provision that

$$\lim_{E \rightarrow 0} g(E) = g_0$$

where g_0 is the level density parameter obtained from Gilbert and Cameron [9]. The limiting values for $g(E)$ are shown in figure 1.

We define the Pauli correction term [3] by

$$E_{Pauli}(P, H) = [\max(P, H)]^2 / g_0 \quad ;$$

$$A(P, H) = E_{Pauli}(P, H) - [P(P+1) + H(H+1)] / 4g_0 \quad .$$

To evaluate the emission probability, $g(E' = E - S_b - \epsilon)$ appears in the integral of (8) over the emission energy; to avoid adding this complexity to the integration, we use the following scheme:

- define $g' = \max[g(E'_{max}), g_0]$;
- approximate $g \approx g'$ in (12) to perform the integral;
- use $\Psi = (g(E')/g')^{N'}$ as a rejection factor

when a residual is chosen with excitation E' and exciton number N' .

The factor Q_b is defined ([3],[5]) by

$$Q_b = \frac{R_b(P)}{R_b^\infty}$$

where $R_b(P)$ is the statistical average of the quantity

$$\binom{P}{p_b}^{-1} \binom{P_\pi}{\pi_b} \binom{P_\nu}{\nu_b} \quad (13)$$

over those particle-hole states which actually occur, and

$$R_b^\infty = \lim_{P \rightarrow \infty} R_b(P)$$

In the above, P_π and P_ν with $P = P_\pi + P_\nu$ are the number of proton and neutron particles in the emitting state; H_π and H_ν with $H = H_\pi + H_\nu$ are defined similarly for holes. For the emitted particle b , π_b and ν_b are the number of protons and neutrons respectively, with $p_b = \pi_b + \nu_b$. If we let $p_a = \pi_a + \nu_a$ refer to the incident particle, the allowed states may be characterized (for the initial stage) by the following scheme.

- $P = p_a + H$, $H = 1, 2, \dots$, where a is the incident projectile;
- $H_\pi = i$, $i = 0, 1, \dots, H$;
- $H_\nu = H - h_\pi = P - p_a - i$;
- $P_\pi = h_\pi + \pi_a = \pi_a + i$;
- $P_\nu = h_\nu + \nu_a = P - \pi_a - i$.

The above reflects the fact that proton *or* neutron particle-hole pairs are created at each internal transition.

In [5], two different models are proposed for the weighting function over which the statistical average of (13) is to be taken:

$$\mathcal{W}_i = \binom{H}{i} \left(\frac{Z}{A}\right)^i \left(\frac{A-Z}{A}\right)^{H-i} \quad (14)$$

where Z and A are taken for the target nucleus, or

$$\mathcal{W}_i = \binom{H + p_a}{i + \pi_a} \binom{H}{i} \left(\frac{Z}{A}\right)^{2i + \pi_a} \left(\frac{A - Z}{A}\right)^{2H - 2i - \pi_a} \quad (15)$$

where Z and A are taken in the compound system. In either case, we evaluate \mathcal{Q}_b from

$$R_b(P) = \frac{\sum_{i=0}^H \mathcal{W}_i \binom{P_\pi}{\pi_b} \binom{P_\nu}{\nu_b}}{\binom{P}{p_b} \sum_{i=0}^H \mathcal{W}_i} \quad (16)$$

and

$$R_b^\infty = \binom{p_b}{\pi_b} \left(\frac{Z}{A}\right)^{\pi_b} \left(\frac{A - Z}{A}\right)^{\nu_b} . \quad (17)$$

[The limiting form R_b^∞ may be obtained from the fact that the binomial distribution approaches a normal distribution for a large number of degrees of freedom and by using the limiting forms of the binomial coefficient.] At the present time, we consider the choice of a weighting function (14) or (15) to be an open question. Furthermore, for second-stage and subsequent emission, we will make the approximation that $\mathcal{Q}_b \approx 1$.

The emission rate $W_b(C, E)$ is obtained by integrating (8) with the insertion of (11) and (12):

$$\begin{aligned} W_b(C, E) &= \mathcal{F}_b(C, E) \int_{\epsilon_{cb}}^{\epsilon_{max}} (\epsilon + \beta_b) [\epsilon_{max} - \epsilon]^{N'-1} d\epsilon \\ &= \mathcal{F}_b(C, E) \mathcal{I}_b(C, E) \end{aligned} \quad (18)$$

where

$$\begin{aligned} N' &= N - p_b \\ \epsilon_{max} &= E - S_b - A(P - p_b, H) \end{aligned}$$

and

$$\mathcal{F}_b(C, E) = \frac{(2s_b + 1) \mu_b \alpha_b \tilde{\sigma}_g g^{N'} \mathcal{Q}_b}{\pi^2 \hbar^3 \omega(C, E) (P - p_b)! H! (N' - 1)!} .$$

The integral in (18) is just

$$\begin{aligned} \mathcal{I}_b(C, E) &= (\epsilon_{max} - \epsilon_{cb})^{N'} \left[\frac{\epsilon_{max} + \beta_b}{N'} - \frac{\epsilon_{max} - \epsilon_{cb}}{N' + 1} \right] \\ &= \frac{(\epsilon_{max} - \epsilon_{cb})^{N'+1}}{N'(N' + 1)} \text{ for charged particles} \\ &= \frac{\epsilon_{max}^{N'+1}}{N'(N' + 1)} \left[1 + \frac{(N' + 1)\beta}{\epsilon_{max}} \right] \text{ for neutrons} . \end{aligned}$$

The Internal Transition Rate

In evaluating the forward internal transition rate $\lambda^+(C, E)$, we follow the practice of GNASH [4]:

$$\lambda^+(C, E) = \frac{2\pi}{\hbar} |M^2| \frac{g^3[E - E_{\text{pauli}}(P + 1, H + 1)]^2}{2(N + 1)} \quad (19)$$

where the level density parameters (at excitation energy E and at zero excitation) are evaluated in the emitting nucleus. The matrix element is parameterized (see references [4] and [5]) by

$$\begin{aligned} |M^2| &= \frac{kN}{A^3 E} \left[\frac{E/N}{7\text{MeV}} \frac{E/N}{2\text{MeV}} \right]^{1/2} && \text{for } E/N < 2 \text{ MeV}, \\ &= \frac{kN}{A^3 E} \left[\frac{E/N}{7\text{MeV}} \right]^{1/2} && \text{for } 2 \text{ MeV} \leq E/N < 7 \text{ MeV}, \\ &= \frac{kN}{A^3 E} && \text{for } 7 \text{ MeV} \leq E/N < 15 \text{ MeV}, \\ &= \frac{kN}{A^3 E} \left[\frac{15\text{MeV}}{E/N} \right]^{1/2} && \text{for } 15 \text{ MeV} \leq E/N. \end{aligned}$$

The constant k is taken to be 135 MeV^3 [5]. Using the same matrix element, the backward internal transition rate $\lambda^-(C, E)$ is given by

$$\begin{aligned} \lambda^-(C, E) &= \frac{2\pi}{\hbar} |M^2| \frac{gPH(N - 2)}{2} \\ &\times \left[1 - \frac{(N - 1)(P - 1)(P - 2) + (H - 1)(H - 2)}{(N - 2)8g[E - E_{\text{pauli}}(P, H)]} \right] \end{aligned} \quad (20)$$

By comparing equations 19 and 20, and using the estimate for the equilibrium exciton number M_{max} given by equation 23 below, we may note that

$$\frac{\lambda^+}{\lambda^-} \sim \left(\frac{N}{N_{\text{max}}} \right)^4$$

Thus we are justified in taking

$$\frac{\lambda^+}{\lambda^-} \ll 1$$

for the low exciton number states from which the bulk of the emission arises.

Selecting the Transition and the Emission Energy

From equations 18 and 19, we may calculate the transition time

$$\tau(C, E) = [\lambda^+(C, E) + \sum_b W_b(C, E)]^{-1}$$

and consequently the forward internal transition probability

$$P^+ = \lambda^+ \tau \quad (21)$$

and the particle emission probabilities

$$P_b = W_b \tau \quad (22)$$

The probabilities of (21) and (22) then define a discrete distribution which is sampled to select the transition type.

If the internal transition is chosen, the state of the system is redefined and a new step is initiated as discussed above. If the new exciton number for the system exceeds the maximum N_{max} , the preequilibrium calculation is terminated. Following [6], we define

$$N_{max} = \left[\frac{8}{5} g E \right]^{1/2} \quad (23)$$

which allows internal transitions (and possible particle emission) to proceed until the exciton number approaches the equilibrium value, at which point emission is more efficiently treated by the evaporation model.

If a particle transition b is selected, then the emission energy ϵ must be sampled from the distribution

$$p_b(\epsilon, C, E) = \frac{(\epsilon + \beta_b)[\epsilon_{max} - \epsilon]^{N'-1}}{\mathcal{I}_b(C, E)}$$

over the range $\epsilon_{cb} \leq \epsilon \leq \epsilon_{max}$. For charged particles, $\beta_b = -\epsilon_{cb}$ so that the transformation

$$\epsilon = \epsilon_{max} - (\epsilon_{max} - \epsilon_{cb})x \quad (24)$$

allows us to sample x from the beta distribution

$$p_b(x) = B_{(N',2)}(x) = N'(N' + 1)x^{N'-1}(1-x) \quad .$$

For neutrons, $\epsilon_{cb} = 0$, so that the above transformation (24) leads to

$$p_n(x) = pB_{(N',1)}(x) + (1-p)B_{(N',2)}(x)$$

with

$$p = \frac{\beta_n}{\beta_n + \frac{\epsilon_{max}}{N'+1}}$$

and

$$B_{(N',1)}(x) = N' x^{N'-1} \quad .$$

Consequently, with probability p , x is sampled from the distribution $B_{(N',1)}(x)$, and, with probability $1 - p$, x is sampled from the distribution $B_{(N',2)}(x)$. Once x is obtained, the emission energy ϵ is obtained from (24).

Having found the emitted particle type and the emission energy, the rejection factors $\Phi_b(\epsilon)$ and Ψ defined above must be applied. Choosing a random number r uniformly $0 < r < 1$, the selection is rejected whenever

$$r > \Phi_b(\epsilon)\Psi$$

and the entire sampling is repeated.

Selecting the Emission Angles

The emission of the *second* and subsequent particles from the compound nucleus is treated as isotropic in the COM; the assumption is made that memory of the incident particle direction is lost after the emission of one particle. However, this is not the case for first stage emission. A parameterization of the angular distribution for first stage emission, based on an analysis of experimental data, has been provided by Kalbach [10].

As described in reference [10], the probability distribution for $\mu = \cos \theta$ is given by

$$p(\mu) = \frac{a}{2 \sinh a} [\cosh a\mu + F_{msd} \sinh a\mu] \quad (25)$$

where θ is the emission angle with respect to the direction of the incident particle. The quantity a is determined by the Kalbach parameterization [10]. The parameter F_{msd} is defined [5] as that fraction of the strength of the emitting state which arises *only* from unbound states in the present and all previous exciton configurations. With the more complex preequilibrium model of reference [5], F_{msd} may be calculated; in our model, it must be supplied. In GNASH [4], $F_{msd} \equiv 1$. In HETC, the completion of an intranuclear cascade is equivalent to saying that the system has reached a “bound” configuration; a subsequent MPM phase would then have $F_{msd} \equiv 0$.

For use in our test code PREEQ1, we assume that F_{msd} decreases geometrically from $F_{msd} = 1$ in the initial configuration with exciton number N_0 to $F_{msd} = f = 0.1$ at the equilibrium exciton number N_{max} of equation 23:

$$F_{msd} = f^x \quad (26)$$

where

$$x = \frac{N - N_0}{N_{max} - N_0} \quad .$$

We note that the above assumption is purely arbitrary and is a candidate for further effort in model development.

Calculations with PREEQ1

The code PREEQ1 performs the Monte Carlo multistage preequilibrium calculation according to the model described above. Executing interactively, the user must input the projectile type (n, p, d, t, τ , or α), the target nucleus (Z,A), the projectile laboratory kinetic energy (MeV), and the number of histories (interactions) to be run. In addition, the user has some choice of options.

- The user may enter a reaction cross section to normalize the output, or allow the code to calculate a reaction cross section according to equation 9.
- The user may input a fixed number for the maximum emitting exciton state or use the default expressed by equation 23.
- The user may enter a minimum emission probability below which the history terminates or use the default (0.001).
- The user has a choice of calculating Q_b with equation 14 (the default), with equation 15, or setting $Q_b \equiv 1$.
- The user may optionally include the *backward* internal transition in the random walk process, according to equation 20 (but the running time may approach infinity if the nuclear system is allowed to approach equilibrium).
- The user may vary the parameter f used to calculate F_{msd} with equation 26; the default is $f = 0.1$. Using $f = 0$ implies $F_{msd} = 1$ for the first exciton state and $F_{msd} = 0$ for the higher exciton states.
- The user may also use models for the level density parameter other than the default model described above. The other choices are the model originally used by the evaporation model in HETC [11] and an alternative more recently developed for use in HETC [12].

The user also has a choice of short or long printed and plotted output; the long output includes the calculated angular distributions for emitted neutrons and protons.

The calculated reaction and particle emission cross sections of four sample cases are illustrated in table 1. The projectile energy in each case was 100 MeV and the default options were used. Each calculation included 100,000 interactions. For the cases with the incident proton, the angle-integrated particle emission spectra are displayed in figures 2 and 3. The component as well as the total emission for protons and neutrons in these cases is illustrated in figures 4 through 7. The first step emission shown is the component coming only from the lowest exciton state (2p,1h) in the first stage. The total first stage and second stage emission are also shown.

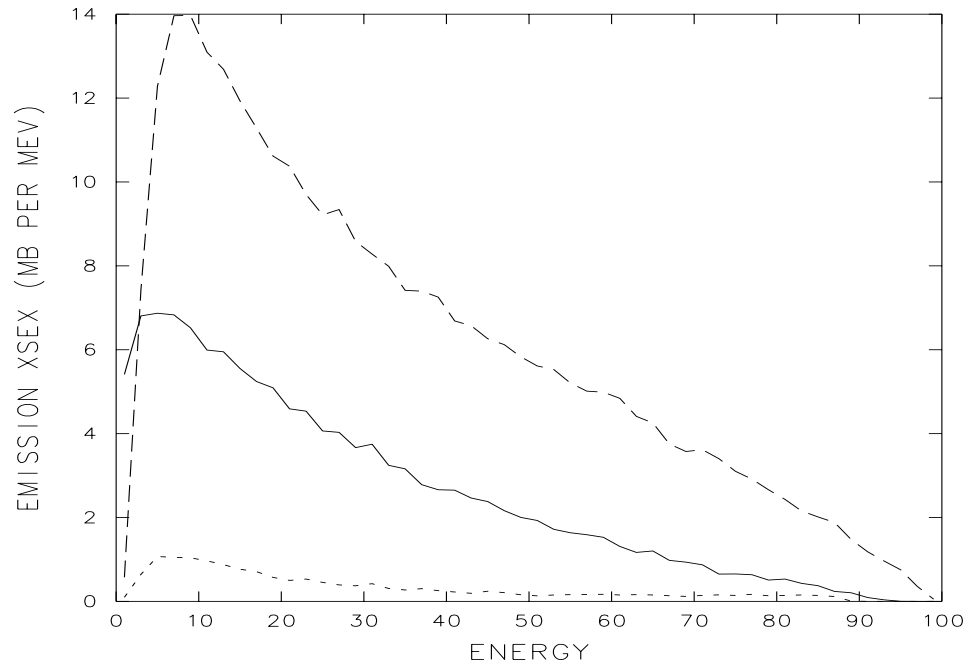


Figure 2: Emission spectrum for $p + {}^{27}\text{Al}$ at 100 MeV. Solid line – neutrons; dashed line – protons; dotted line – deuterons.

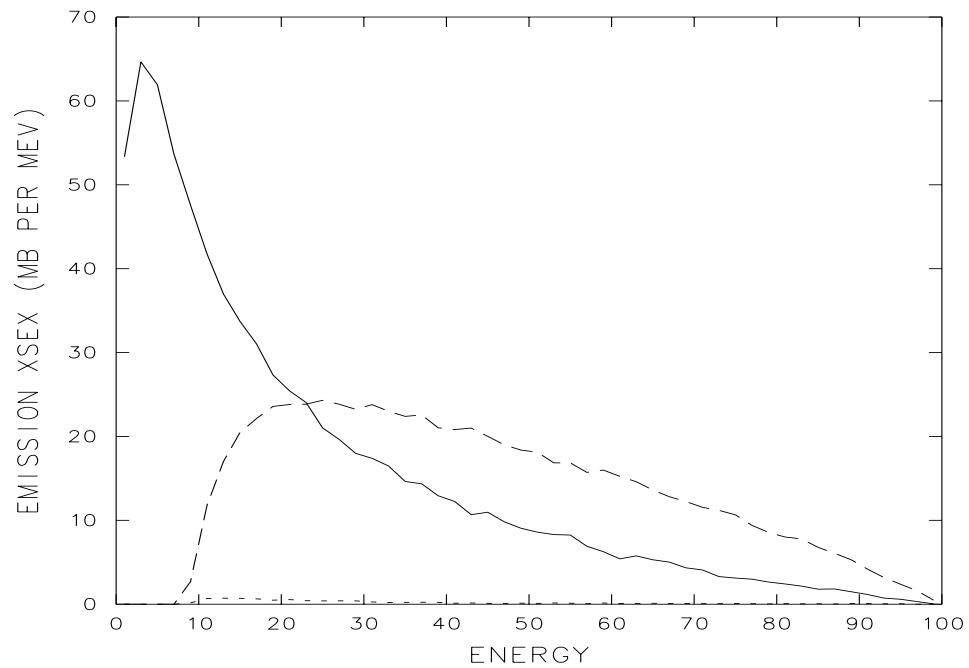


Figure 3: Emission spectrum for $p + {}^{238}\text{U}$ at 100 MeV. Lines defined as in figure 2.

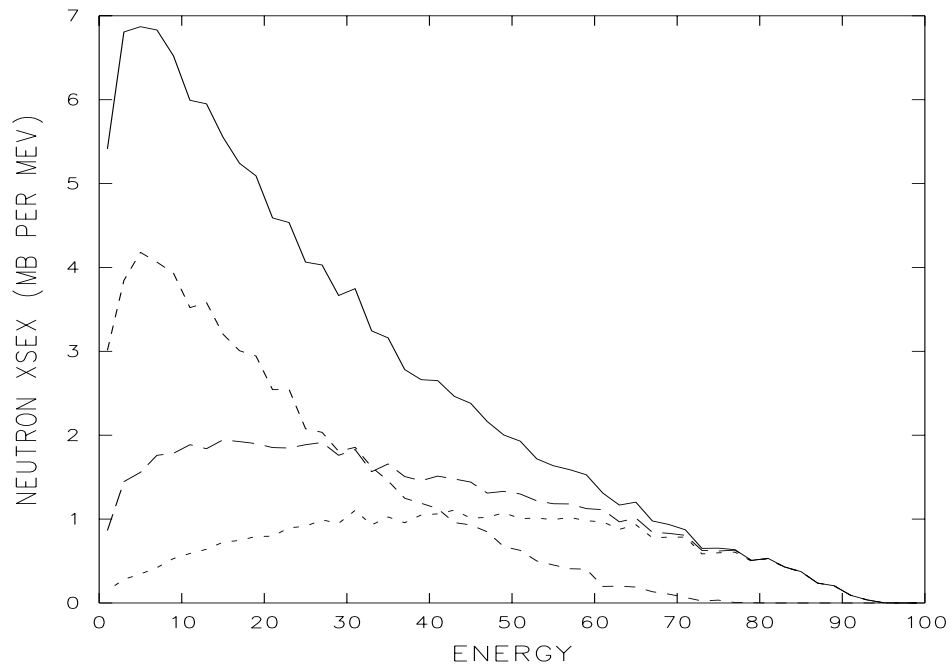


Figure 4: Neutron spectrum for $p + {}^{27}\text{Al}$ at 100 MeV. Solid line – total emission; dotted line – first *step*; long dashed line – total first stage; short dashed line – second stage .

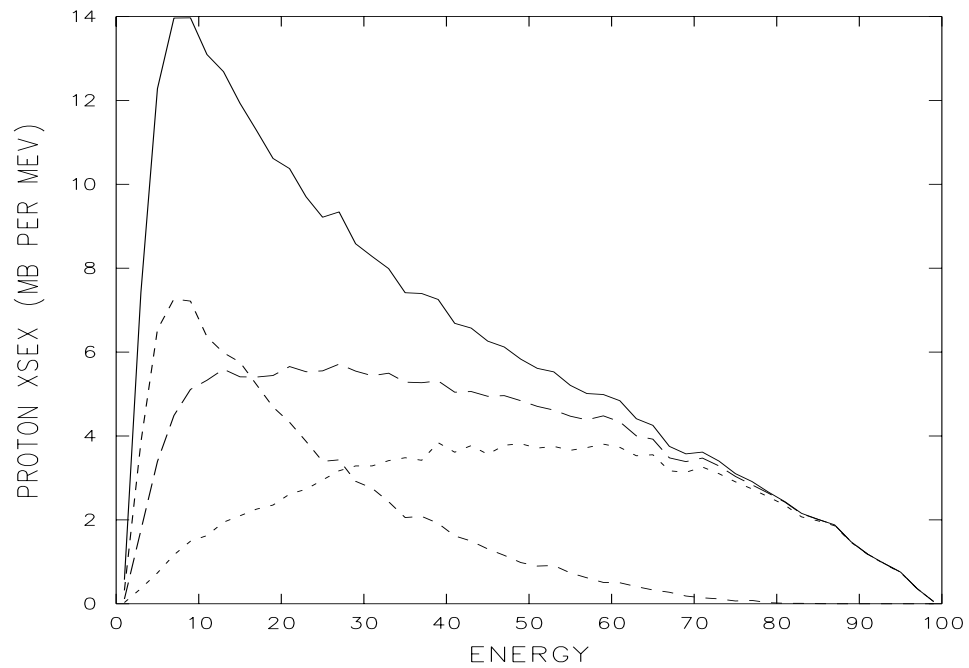


Figure 5: Proton spectrum for $p + {}^{27}\text{Al}$ at 100 MeV. Lines defined as in figure 4.

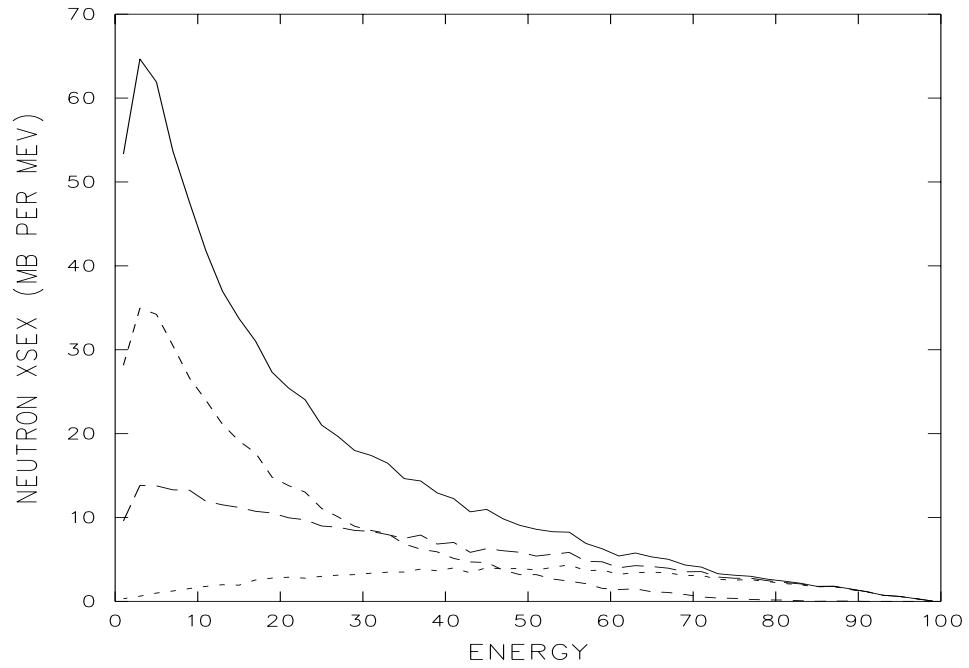


Figure 6: Neutron spectrum for $p + {}^{238}\text{U}$ at 100 MeV. Lines defined as in figure 4.

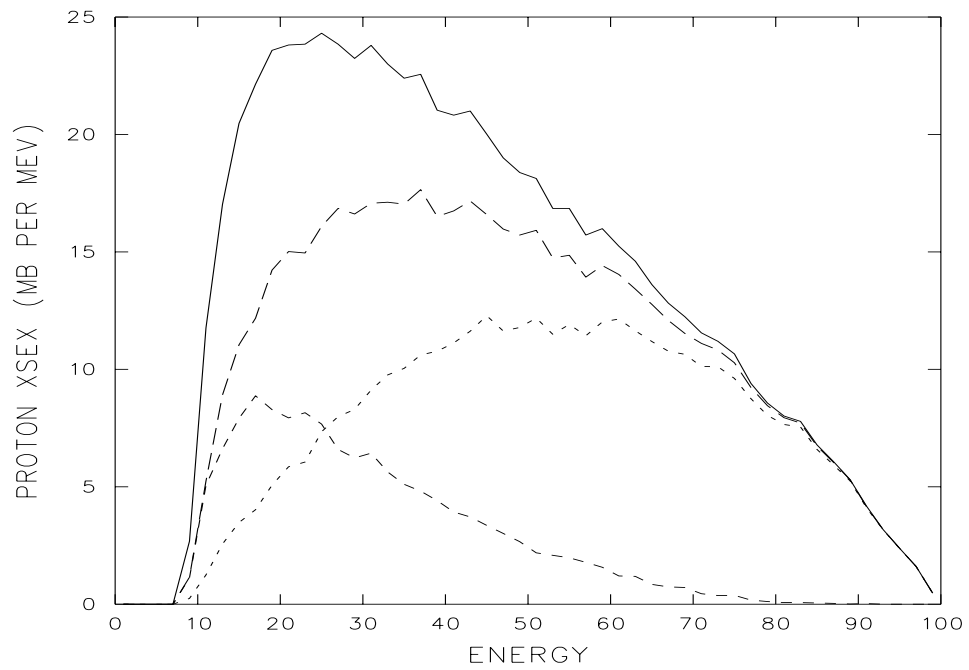


Figure 7: Proton spectrum for $p + {}^{238}\text{U}$ at 100 MeV. Lines defined as in figure 4.

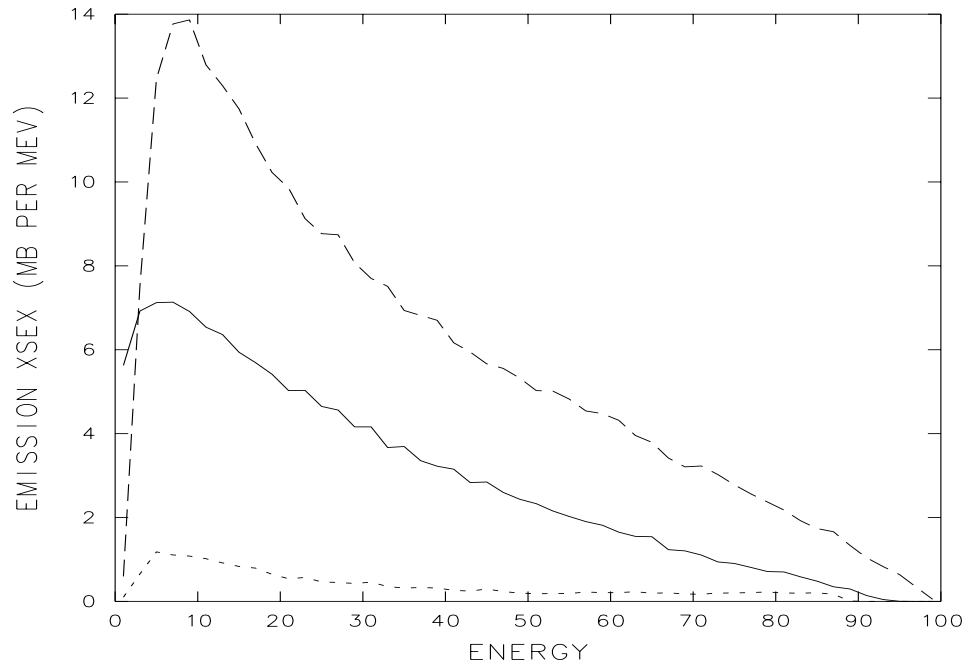


Figure 8: Emission spectrum for $p + {}^{27}\text{Al}$ at 100 MeV, with Q_b calculated with equation 15. Lines defined as in figure 2.

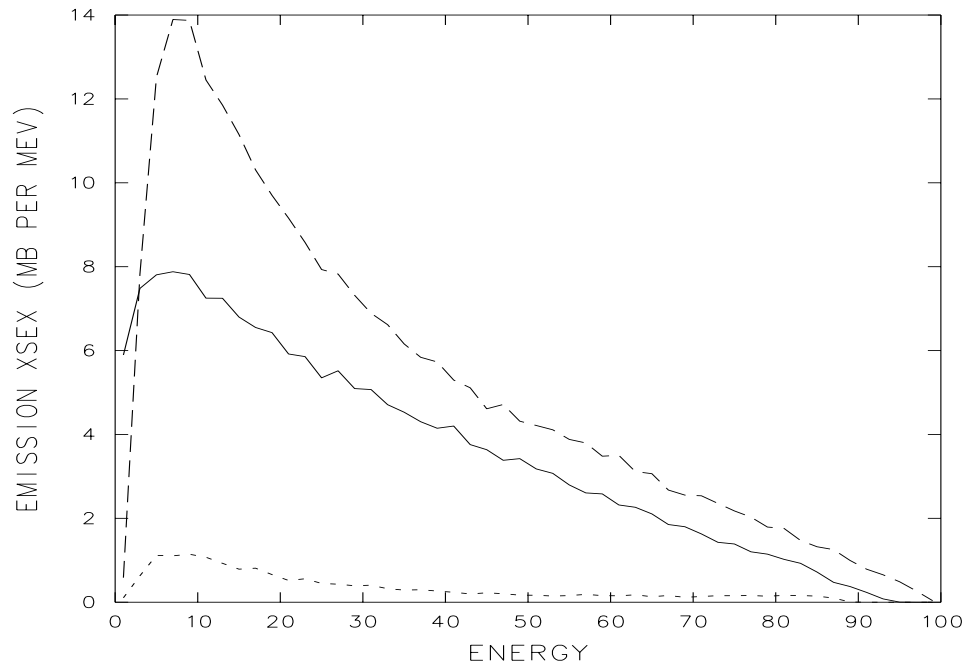


Figure 9: Emission spectrum for $p + {}^{27}\text{Al}$ at 100 MeV, with $Q_b \equiv 1$. Lines defined as in figure 2.

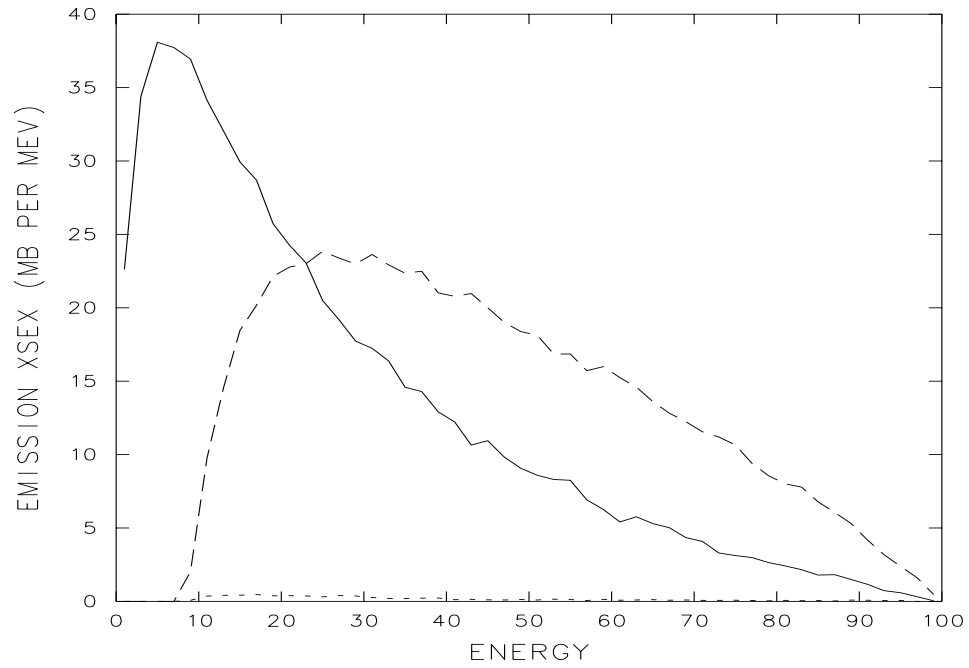


Figure 10: Emission spectrum for $p + ^{238}\text{U}$ at 100 MeV, calculated with $N_{max} = 13$. Lines defined as in figure 3.

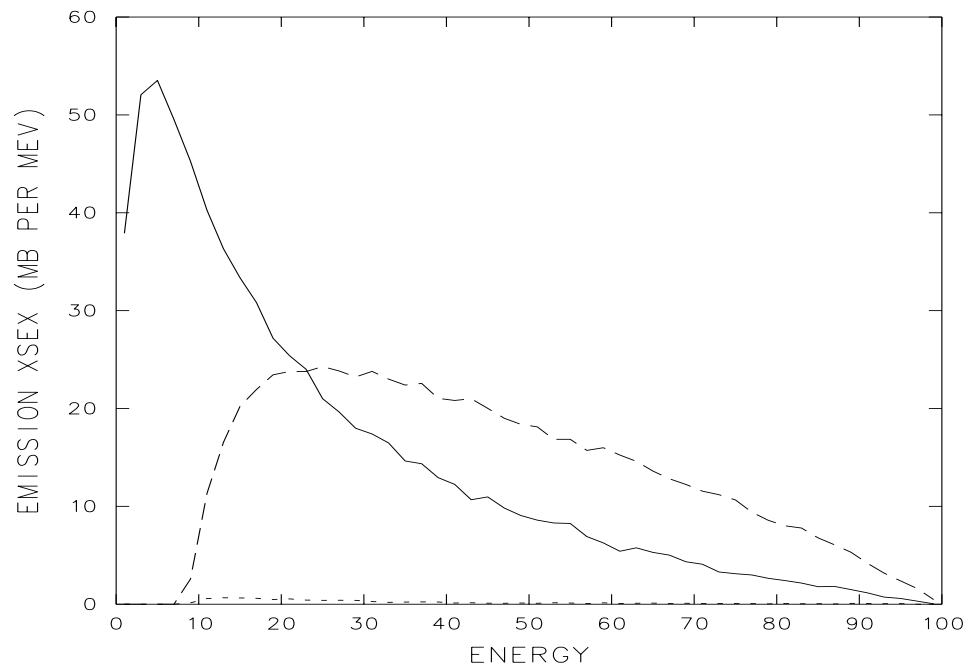


Figure 11: Emission spectrum for $p + ^{238}\text{U}$ at 100 MeV, calculated with $N_{max} = 23$. Lines defined as in figure 3.

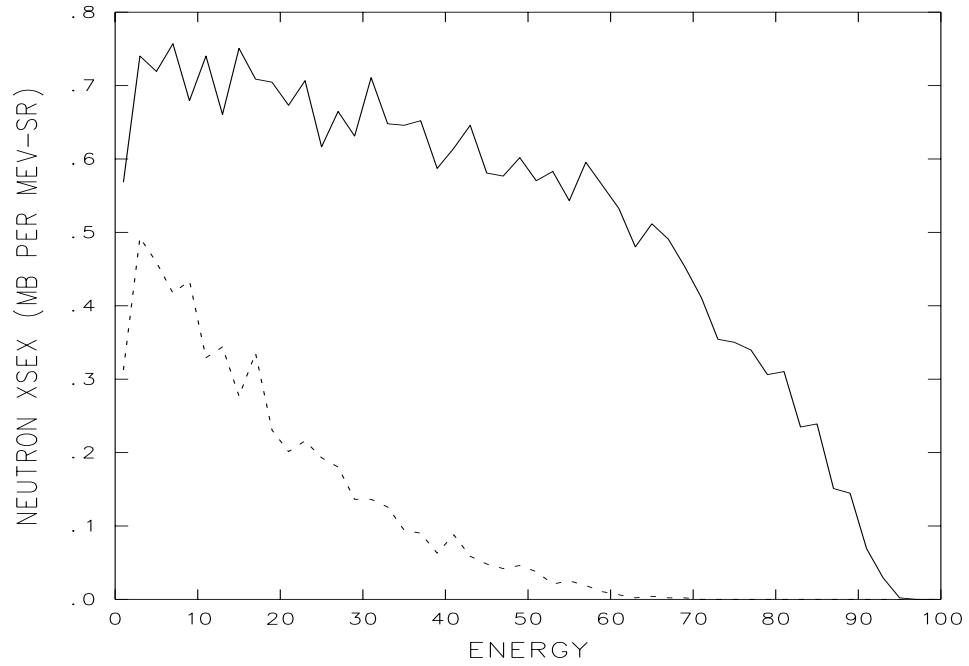


Figure 12: Differential neutron spectrum for $p+^{27}\text{Al}$ at 100 MeV with $f = 1$ in equation 26. Solid line for $\bar{\mu} = +0.9$, dashed line for $\bar{\mu} = -0.9$.

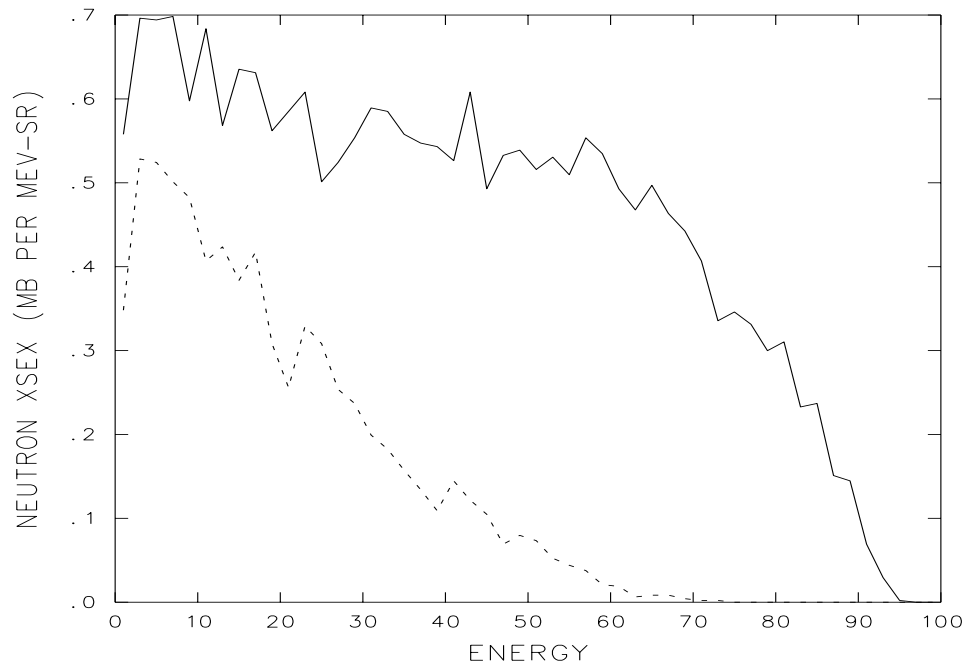


Figure 13: Differential neutron spectrum for $p+^{27}\text{Al}$ at 100 MeV with $f = 0$ in equation 26. Lines defined as in figure 12.

	$p + {}^{27}\text{Al}$	$n + {}^{27}\text{Al}$	$p + {}^{238}\text{U}$	$n + {}^{238}\text{U}$
Reaction	527.06	544.34	1757.1	2050.8
Neutron	127.63	275.44	781.5	1346.2
Proton	301.01	170.43	677.9	385.6
Deuteron	15.42	17.28	9.1	8.8
Triton	0.44	0.77	0.3	0.3
Tau	0.84	0.34	0.1	0.1
Alpha	0.43	0.32	0.1	0.2

Table 1: Calculated reaction and preequilibrium emission cross sections (mb) for sample cases at 100 MeV projectile energy.

By comparing figures 2, 8, and 9, we may observe the effect of the various methods for computing the factor Q_b . The “memory” of the projectile type is most strongly retained by calculating Q_b with equation 14 (figure 2); it is noticeably less so when calculated with equation 15 (figure 8). For contrast, figure 9 shows the spectrum as calculated with no “memory” ($Q_b \equiv 1$).

In our sample case for $p + {}^{238}\text{U}$ at 100 MeV incident energy (figure 3), the computed equilibrium exciton number is 53.6; thus first stage emission is allowed through exciton number $N_{max} = 53$. In figure 10, we see the effect of restricting the calculation to exciton number $N_{max} + 13$; figure 11 illustrates the effect of truncation at $N_{max} = 23$. The low energy neutron spectrum is strongly sensitive to the choice of N_{max} .

As mentioned above, the choice of the parameter F_{msd} for calculating the angular distribution for emitted particles has been made quite arbitrarily at the present time ($f = 0.1$ in equation 26). To illustrate the effect of the parameter f , two extreme cases are shown in figures 12 and 13 where we see the neutron spectrum for the case $p + {}^{27}\text{Al}$ at 100 MeV incident energy averaged over angular intervals $0.8 \leq \mu \leq 1.0$ and $-1.0 \leq \mu \leq -0.8$. For figure 12, $f = 1$ so $F_{msd} \equiv 1$, which leads to the maximum emission in the forward direction and the minimum in the backward. For figure 13, we have taken $f = 0$, so that $F_{msd} = 1$ *only* for the lowest ($N = 3$) exciton state and $F_{msd} = 0$ for all other first stage emission. For this particular case, the effect on the spectrum in the backward direction is as large as 20%.

Summary

In the sections above, we have outlined the the necessary components for the development of a Monte Carlo multistage preequilibrium model code. From them, we have developed a stand-alone MPM Monte Carlo code PREEQ1 that largely parallels the methodology used in GNASH [4] and has allowed us to test the implementation of the various components. Furthermore, PREEQ1 provides an ideal test vehicle for alternative algorithms and new theoretical methods. The stand-alone code will provide the subroutines for the implementation of the preequilibrium model into HETC.

As noted above, the question of the estimation of inverse reaction cross sections is still open and will be treated in future development. However, the parameterization by Chatterjee [13] appears to offer a complete and applicable formulation.

The remaining theoretical questions, which will be addressed in a subsequent paper, concern the interface between the intranuclear cascade model and the MPM and the interface between the MPM and the evaporation model. Our experience gained with the stand-alone code will help us in this effort.

References

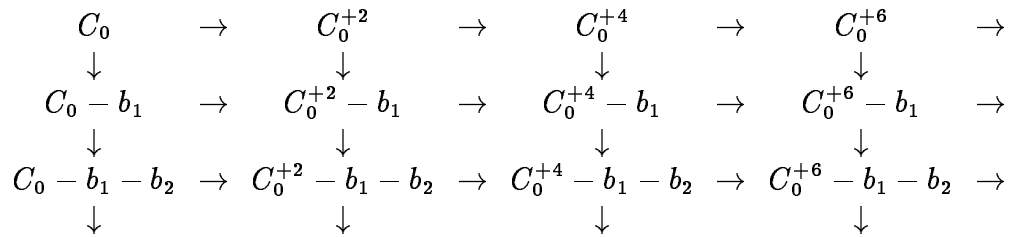
- [1] Radiation Shielding Information Center, "HETC: Monte Carlo High-Energy Nucleon-Meson Transport Code", CCC-178, Oak Ridge National Laboratory (1977).
- [2] F. J. Luider, "Pre-equilibrium Theory and Slaves of the Master Equation", ECN-17, Netherlands Energy Research Foundation ECN (1977).
- [3] C. Kalbach, *Zeitschrift für Physik A 283* (1977), p. 401.
- [4] E. D. Arthur, "The GNASH Preequilibrium-Statistical Model Code", LA-UR-88-382, Los Alamos National Laboratory (1988).
- [5] C. Kalbach, "PRECO-D2: Program for Calculating Preequilibrium and Direct Reaction Double Differential Cross Sections", LA-10248-MS, Los Alamos National Laboratory (1985).
- [6] H. Gruppelaar and J. M. Akkermans, "The GRAPE Code System for the Calculation of Precompound and Compound Nuclear Reactions – GRYPHON Code Description and Manual", ECN-164, Netherlands Energy Research Foundation ECN (1985).
- [7] F.C.Williams, *Nuclear Physics A166* (1971), p. 231.

- [8] A. V. Ignatyuk, G. N. Smirenkin, and A. S. Tishin, *Sov. J. Nucl. Phys.* *21* (1975), p. 256.
- [9] A. Gilbert and A. G. W. Cameron, *Can. J. Physics* *43* (1965), p. 1446.
- [10] C. Kalbach, "Systematics of Continuum Angular Distributions: Extensions to Higher Energies", LA-UR-87-4139, Los Alamos National Laboratory (1987).
- [11] L. Dresner, "EVAP – A Fortran Program for Calculating the Evaporation of Various Particles from Excited Compound Nuclei", ORNL-TM-196, Oak Ridge National Laboratory (1962).
- [12] P. Cloth et al., "The KFA-Version of the High-Energy Transport Code HETC and the Generalized Evaluation Code SIMPEL", Jül-Spez-196, Kernforschungsanlage Jülich GmbH (1983).
- [13] A. Chatterjee, K. H. N. Murthy, and S. K. Gupta, *Pramāna* *16* (1981), p. 391.

Appendices

Analytical Results

As an addendum to the above discussion, we include some results that may be derived from the above which are of interest in performing analytical MPM calculations but which are not needed in a Monte Carlo implementation (although they illustrate features of the random walk). In the diagram below, we illustrate the possible paths for the evolution of the nuclear system.



The initial state C_0 evolves by transition to the states $C_0 + 2k$ (labeled as C_0^{+2k} in the diagram) within the first stage. Emission of a particle b_1 in the first stage from state $C_0 + 2k$ leads to the state $C_0 + 2k - b_1$ (with energy $E' = E_0 - S_{b_1} - \epsilon_{b_1}$). Similarly, all possible states which may occur in the third stage may be labeled by $C_0 + 2k - b_1 - b_2$ where b_2 is the particle emitted in the second stage; the energy would then be computed from $E' = E_0 - S_{b_1} - \epsilon_{b_1} - S_{b_2} - \epsilon_{b_2}$. [Note that this counting scheme will include states

which do not emit ($P = 0$) and some that are nonphysical ($P < 0$); this will cause no problem, since in the former case, $w_b \equiv 0$, while in the latter, the function $Q_\nu \equiv 0$.]

Let us define a *depletion factor* $D_{jk}(C, E)$ by

$$D_{jk}(C, E) = \prod_{i=j}^{k-1} \lambda^+(C + 2i, E) \tau(C + 2i, E) \text{ for } k > j$$

$$D_{jj}(C, E) \equiv 1 \text{ for } k = j$$

where the following relationship holds:

$$D_{ij}(C, E) D_{jk}(C, E) = D_{ik}(C, E) \quad .$$

To compact our notation somewhat, let us also define w_b^* by

$$w_b^*(\epsilon, C, E) = w_b(\epsilon, C, E) \tau(C, E) \quad .$$

From equations 4 and 5, we obtain

$$Q_1(C_0 + 2k, E) = D_{0k}(C_0, E) \delta(E - E_0)$$

so that the differential cross section for b coming from the *first stage* is just

$$\begin{aligned} \left(\frac{d\sigma_b}{d\epsilon} \right)_1 &= \sigma_R \sum_{k=0}^{k_{max}} \int w_b^*(\epsilon, C_0 + 2k, E) Q_1(C_0 + 2k, E) dE \\ &= \sigma_R \sum_{k=0}^{k_{max}} w_b^*(\epsilon, C_0 + 2k, E_0) D_{0k}(C_0, E_0) \end{aligned}$$

We can reduce equation 6 to

$$Q_\nu(C_\nu + 2k, E) = \sum_{i=0}^k \sum_b D_{ik}(C_\nu, E)$$

$$\times \int w_b^*(E' - S_b - E, C_\nu + b + 2i, E') Q_{\nu-1}(C_\nu + b + 2i, E') dE'$$

where the summation is over all the potential precursor states in the $\nu - 1$ stage. If we apply this to the second stage, we get

$$Q_2(C_0 - b_1 + 2k, E) = \sum_{i=0}^k D_{ik}(C_0 - b_1, E) w_b^*(E_0 - S_{b_1} - E, C_0 + 2i, E_0) D_{0i}(C_0, E_0)$$

which leads to the following form for the differential cross section for b coming from the *second stage*:

$$\begin{aligned} \left(\frac{d\sigma_b}{d\epsilon}\right)_2 &= \sigma_R \sum_{k=0}^{k_{max}} \sum_{i=0}^k \sum_{b_1} \int dE \\ &\times w_b^*(\epsilon, C_0 - b_1 + 2k, E) D_{ik}(C_0 - b_1, E) \\ &\times w_{b_1}^*(E_0 - S_{b_1} - E, C_0 + 2i, E_0) D_{0i}(C_0, E_0) \quad . \end{aligned}$$

With somewhat more labor, the differential cross section in the *third stage* is

$$\begin{aligned} \left(\frac{d\sigma_b}{d\epsilon}\right)_3 &= \sigma_R \sum_{k=0}^{k_{max}} \sum_{j=0}^k \sum_{i=0}^j \sum_{b_2} \sum_{b_1} \int \int dE' dE \\ &\times w_b^*(\epsilon, C_0 - b_1 - b_2 + 2k, E') D_{jk}(C_0 - b_1 - b_2, E') \\ &\times w_{b_2}^*(E - S_{b_2} - E', C_0 - b_1 + 2j, E) D_{ij}(C_0 - b_1, E) \\ &\times w_{b_1}^*(E_0 - S_{b_1} - E, C_0 + 2i, E_0) D_{0i}(C_0, E_0) \quad . \end{aligned}$$

Evaluation of $R_b(P)$

When the weighting function \mathcal{W}_i is the binomial distribution, as in equation 14, then the factors $R_b(P)$ may be directly evaluated. The identity

$$\sum \binom{H}{i} \rho^i (1-\rho)^{H-i} \binom{i}{k} \binom{H-i}{l} = \binom{k+l}{k} \binom{H}{k+l} \rho^k (1-\rho)^l$$

is useful in performing the evaluation. Using $P = H + p_a$ and $\rho = Z/A$, we obtain the following expressions.

$$\begin{aligned} R_n(P) &= \frac{H(1-\rho) + \nu_a}{P} \\ R_p(P) &= \frac{H\rho + \pi_a}{P} \\ R_d(P) &= \frac{2\{H(H-1)\rho(1-\rho) + H[\nu_a\rho + \pi_a(1-\rho)] + \pi_a\nu_a\}}{P(P-1)} \\ R_t(P) &= \frac{3}{P(P-1)(P-2)} \left\{ H(H-1)(H-2)\rho(1-\rho)^2 \right. \\ &\quad \left. + H(H-1)[2\nu_a\rho(1-\rho) + \pi_a(1-\rho)^2] \right. \\ &\quad \left. + H[\nu_a(\nu_a-1)\rho + 2\pi_a\nu_a(1-\rho)] + \pi_a\nu_a(\nu_a-1) \right\} \\ R_r(P) &= \frac{3}{P(P-1)(P-2)} \left\{ H(H-1)(H-2)\rho^2(1-\rho) \right. \end{aligned}$$

$$\begin{aligned}
& +H(H-1)[2\pi_a\rho(1-\rho) + \nu_a\rho^2] \\
& +H[\pi_a(\pi_a-1)(1-\rho) + 2\pi_a\nu_a\rho] + \pi_a(\pi_a-1)\nu_a\} \\
R_\alpha(P) = & \frac{6}{P(P-1)(P-2)(P-3)} \{H(H-1)(H-2)(H-3)\rho^2(1-\rho)^2 \\
& +2H(H-1)(H-2)[\pi_a\rho(1-\rho)^2 + \nu_a\rho^2(1-\rho)] \\
& +H(H-1)[\pi_a(\pi_a-1)(1-\rho)^2 + 4\pi_a\nu_a\rho(1-\rho) + \nu_a(\nu_a-1)\rho^2] \\
& +2H[\pi_a\nu_a(\nu_a-1)\rho + \pi_a(\pi_a-1)\nu(1-\rho)] \\
& +\pi_a(\pi_a-1)\nu_a(\nu_a-1)\}
\end{aligned}$$